The ^{4}He abundance in the metal-deficient blue compact dwarf galaxies Tol 1214–277 and Tol 65[1]

Yuri I. Izotov[2]

Main Astronomical Observatory, National Academy of Sciences of Ukraine, 03680, Kyiv, Ukraine

izotov@mao.kiev.ua

Frederic H. Chaffee

W. M. Keck Observatory, 65-1120 Mamalahoa Hwy., Kamuela, HI 96743, USA

fchaffee@keck.hawaii.edu

and

Richard F. Green

National Optical Astronomy Observatory, Tucson, AZ 85726, USA

rgreen@noao.edu

ABSTRACT

We present high-quality Keck telescope spectroscopic observations of the two metal-deficient blue compact dwarf (BCD) galaxies Tol 1214–277 and Tol 65. These data are used to derive the heavy-element and helium abundances. We find that the oxygen abundances in Tol 1214–277 and Tol 65 are the same, 12 + log O/H = 7.54 ± 0.01, or $Z_\odot/24$, despite the different ionization conditions in these galaxies. The nitrogen-to-oxygen abundance ratio in both galaxies is log N/O = –1.64±0.02 and lies in the narrow range found for the other most metal-deficient BCDs. We use the five strongest He I emission lines $\lambda\lambda$3889, 4471, 5876, 6678 and 7065, to correct self-consistently their intensities for collisional and fluorescent enhancement mechanisms and to derive the ^{4}He abundance. Underlying stellar absorption is found to be important for the He I λ4471 emission line in both galaxies, being larger in Tol 65. The weighted ^{4}He mass fractions in Tol 1214–277 and Tol 65 are respectively $Y = 0.2458 \pm 0.0039$ and 0.2410 ± 0.0050 when the three He I emission lines, $\lambda\lambda$4471, 5876 and 6678 Å, are used, and are, respectively, 0.2466 ± 0.0043 and 0.2463 ± 0.0057 when the He I 4471

Å emission line is excluded. These values are in very good agreement with recent measurements of the ^{4}He mass fraction in others of the most metal-deficient BCDs by Izotov and coworkers. We find that the combined effect of the systematic uncertainties due to the underlying He I stellar absorption lines, ionization and temperature structure of the H II region and collisional excitation of the hydrogen emission lines is likely small, not exceeding $\sim 2\%$ (the error is 2σ). Our results support the validity of the standard big bang model of nucleosynthesis.

Subject headings: galaxies: abundances — galaxies: irregular — galaxies: ISM — H II regions — ISM: abundances — galaxies: individual (Tol 1214–277, Tol 65)

1. Introduction

In the standard big bang model of nucleosynthesis (SBBN), the light isotopes D, ^{3}He, ^{4}He and ^{7}Li were produced by nuclear reactions a few minutes after the birth of the Universe. Given the number of light neutrino species $N_\nu = 3$ and the neutron lifetime, the abundances of these light elements depend on one cosmological parameter only, the baryon-to-photon ratio η, which in turn is directly related to the density of ordinary baryonic matter Ω_b.

The ideal objects for determination of the primordial helium abundance are blue compact dwarf (BCD) galaxies. These dwarf systems are the least chemically evolved galaxies known, so they contain very little helium manufactured by stars after the big bang. Because the big bang production of ^{4}He is relatively insensitive to the density of matter, the primordial abundance of ^{4}He must be determined to very high precision (better than a few percent relative accuracy) in order to put useful constraints on $\Omega_{\rm b}$. This precision can be achieved with very high signal-to-noise ratio optical spectra of BCDs. These BCDs are undergoing intense bursts of star formation, giving birth to high excitation supergiant H II regions, which allow an accurate determination of the helium abundance in the ionized gas

[1]The observations reported here were obtained at the W. M. Keck Observatory, which is operated as a scientific partnership among the California Institute of Technology, the University of California, and the National Aeronautics and Space Administration. The Observatory was made possible by the generous financial support of the W. M. Keck Foundation.

[2]Visiting astronomer, National Optical Astronomy Observatory, which is operated by the Association of Universities for Research in Astronomy, Inc. (AURA) under cooperative agreement with the National Science Foundation (NSF).

through the BCD's emission-line spectrum. The primordial helium mass fraction $Y_{\rm p}$ of ^{4}He is usually derived by extrapolating the Y – O/H and Y – N/H correlations to O/H = N/H = 0, as proposed originally by Peimbert & Torres-Peimbert (1974, 1976) and Pagel, Terlevich & Melnick (1986). Many attempts at determining $Y_{\rm p}$ have been made, using these correlations on various samples of dwarf irregulars and BCDs (e.g., Pagel et al. 1992; Izotov, Thuan & Lipovetsky 1994, 1997, hereafter ITL94 and ITL97; Olive, Steigman & Skillman 1997; Izotov & Thuan 1998; Pagel 2000). Another way to infer the primordial ^{4}He abundance is to measure the helium abundance in the most metal-deficient BCDs, which is very close to the primordial value (e.g., Izotov et al. 1999).

Recent $Y_{\rm p}$ determinations made by Izotov & Thuan (1998) and Izotov et al. (1999) resulted in a very narrow range of $Y_{\rm p} \sim 0.244 - 0.245$. They used high signal-to-noise spectroscopic observations of BCDs reduced in a homogeneous way. A self-consistent method was applied to correct He I emission line intensities for the collisional and fluorescent enhancement mechanisms which lead to deviations from the values predicted by recombination theory. The use of several He I lines allows one to discriminate between collisional and fluorescent enhancements which change the line intensities in different ways. It also allows one to estimate the importance of underlying stellar absorption in each galaxy and to improve the precision of the $Y_{\rm p}$ determination through the use of several lines. The details of this approach are discussed by ITL97 and Izotov & Thuan (1998).

Our present study is the continuation of helium abundance determinations in the lowest-metallicity BCDs based on spectroscopic observations with the 10m Keck telescope. Earlier such studies have been done for the BCDs SBS 0335–052 ($Z_\odot/40$, Izotov et al. 1999) and SBS 0940+544 ($Z_\odot/27$, Guseva et al. 2001). We focus here on two southern BCDs, Tol 1214–277 and Tol 65 ≡ Tol 1223–359, the very low metallicity of which ($\sim Z_\odot/25$) has been established by earlier spectroscopic work (Kunth & Sargent 1983; Campbell et al. 1986; Pagel et al. 1992; Masegosa, Moles & Campos-Aguilar 1994; Fricke et al. 2001). The motivation of our work is as follows. First, these galaxies are relatively bright targets for a large telescope which allows the derivation of the ^{4}He abundance with great precision. Second, Tol 1214–277 and Tol 65 are the second and third lowest-metallicity BCDs in the Pagel et al. (1992) sample (after I Zw 18), for which those authors derived very low ^{4}He mass fractions $Y = 0.233$ and 0.231 respectively. Those values are in disagreement with the significantly larger Y's derived in later studies of other very low metallicity BCDs. Third, recently several papers have appeared (e.g., Ballantyne, Ferland & Martin 2000; Viegas, Gruenwald & Viegas 2000; Sauer & Jedamzik 2001; Peimbert, Peimbert & Luridiana 2001; Stasińska & Izotov 2001) where systematic effects on the ^{4}He abundance determination are discussed. Here we estimate the systematic uncertainties for several of the best-observed low-metallicity BCDs, including Tol 1214–277 and Tol 65.

In Sect. 2 we describe the observations and data reduction. Heavy element abundances are derived in Sect. 3. The results of the ^{4}He abundance determination are discussed in Sect. 4. We discuss the systematic uncertainties in ^{4}He abundance determinations in Sect. 5. The summary is in Sect. 6.

2. Observations and data reduction

The Keck II spectroscopic observations of Tol 1214–277 and Tol 65 were carried out on January 9, 2000, with the low-resolution imaging spectrograph (LRIS) (Oke et al. 1995), using the 300 groove mm^{-1} grating, which provides a dispersion 2.52 Å pixel^{-1} and a spectral resolution of about 8 Å in first order. The slit was $1''\times180''$, centered on the brightest central regions and oriented with a position angle P.A. = –19° for Tol 1214–277 and –51° for Tol 65 (Fig. 1). No binning along the spatial axis has been done, yielding a spatial sampling of $0\farcs2$ pixel^{-1}. The total exposure time was 45 min for each galaxy, broken into three 15-min exposures. All exposures were taken at airmasses of 1.7 and 1.8 for Tol 1214–277 and Tol 65, respectively. The seeing was $0\farcs9$. No blocking filter was used. Therefore some second-order contamination is present in the red parts of spectra at wavelengths > 7000Å.

The spectrophotometric standard stars Feige 34 and HZ 44 were observed for flux calibration. Spectra of a Hg-Ne-Ar comparison lamp were obtained before and after each observation to provide the wavelength calibration.

Data reduction of the observations was carried out at the Main Astronomical Observatory of Ukraine using the IRAF software package.[3] This reduction included bias subtraction, cosmic-ray removal and flat-field correction using exposures of a quartz incandescent lamp. After wavelength calibration, night-sky background subtraction, and correction for atmospheric extinction, each frame was calibrated to absolute fluxes. Because both BCDs were observed at large airmasses, the atmospheric differential refraction can be important (Filippenko 1982). This effect is smaller for Tol 1214–277 because of its higher declination and slit position angle close to the parallactic one. To minimize the effect of the atmospheric differential refraction we extracted one-dimensional spectra from large apertures $1'' \times 6\farcs8$ for Tol 1214–277 and $1'' \times 8\farcs4$ for Tol 65. The spectra are shown in Figs. 2 and 3. They are dominated by very strong emission lines. Remarkable spectral features in Tol 1214–277 are the strong nebular He II λ4686 and [Fe V] λ4227 emission lines suggesting a very hard stellar radiation field in the BCD (Fig. 2). The latter line was detected first by Fricke et al.

[3]IRAF: the Image Reduction and Analysis Facility is distributed by the National Optical Astronomy Observatory.

(2001) in the VLT spectrum of Tol 1214–277. This line is absent in the spectrum of Tol 65 where He II λ4686 is also weaker, implying that the radiation in this galaxy is softer.

The fluxes of the nebular lines have been measured by fitting Gaussians to the line profiles. The errors in the line fluxes include the errors in placement of the continuum and those in the Gaussian fitting. We also take into account the errors introduced by uncertainties in the spectral energy distributions of the standard stars. Standard star flux deviations for both Feige 34 and HZ 44 are taken to be 1% (Oke 1990; Bohlin 1996). These 1σ errors have been propagated in calculations of the electron temperature, electron number density and elemental abundances. The observed and extinction-corrected emission line fluxes and observed equivalent widths are shown in Table 1 together with the extinction coefficient $C(\mathrm{H}\beta)$, derived from the decrement of hydrogen emission lines which includes both Milky Way and target galaxy extinction, the absolute flux $F(\mathrm{H}\beta)$ of the Hβ emission line and average equivalent width EW(abs) of the hydrogen absorption lines. The errors of the fluxes and equivalent widths of the emission lines introduced by second-order contamination are relatively small. We estimate this effect by measuring the fluxes of the [O II] λ3727 and [Ne III] λ3868 emission lines in the second order spectra of both galaxies and find that they are respectively $\sim 1.5\%$ and ~ 3 – 4% of those in the first order spectra. This implies that the effect of the second-order contamination is less than 1% at wavelengths shorter 7500Å, smaller than the flux errors of the weak lines seen at 7000 – 7300Å. Therefore, we do not take into account this effect.

3. Heavy element abundances

To derive heavy element abundances, we have followed the procedure detailed in ITL94 and ITL97. We adopted a two-zone photoionized H II region model (Stasińska 1990) including a high-ionization zone with temperature T_{e}(O III), and a low-ionization zone with temperature T_{e}(O II). We have determined T_{e}(O III) from the [O III]λ4363/(λ4959+λ5007) ratio using a five-level atom model. That temperature is used for the derivation of the O^{+2}, Ne^{+2} and Ar^{+3} ionic abundances. To derive T_{e}(O II), we have utilized the relation between T_{e}(O II) and T_{e}(O III) (ITL94), based on a fit to the photoionization models of Stasińska (1990). The temperature T_{e}(O II) is used to derive the O^{+}, N^{+}, S^{+} and Fe^{+} ionic abundances. For Ar^{+2} and S^{+2} we have adopted an electron temperature intermediate between T_{e}(O III) and T_{e}(O II) following the prescriptions of Garnett (1992). The electron number density N_{e}(S II) (Table 2) is derived from the [S II] λ6717/λ6731 ratio. We point out that the flux of the [S II] λ6717 emission line in Tol 1214–277 spectrum is significantly reduced due to coincidence with a night sky absorption line. This artificially low intensity results in a

significant overestimate of N_e(S II). However, the heavy element abundances in low-density H II regions do not depend on N_e. Therefore, the uncertainties in N_e(S II) (Table 2) do not contribute significantly to the error budget of the heavy element abundances.

The oxygen abundance is derived as

$$\frac{O}{H} = \frac{O^+}{H^+} + \frac{O^{+2}}{H^+} + \frac{O^{+3}}{H^+}, \quad (1)$$

where the O^{+3} abundance is derived from the relation

$$\frac{O^{+3}}{O^+ + O^{+2}} = \frac{He^{+2}}{He^+}. \quad (2)$$

Total abundances of other heavy elements were computed after correction for unseen stages of ionization as described in ITL94 and Thuan, Izotov & Lipovetsky (1995).

The abundances of oxygen and other heavy elements obtained in this study for both galaxies are in general agreement with previous studies. Our value for the oxygen abundance in Tol 1214–277, 12 + log (O/H) = 7.54 ± 0.01, compares with values of 7.54±0.04 (Campbell et al. 1986), 7.59±0.05 (Pagel et al. 1992), 7.57±0.01 (Masegosa et al. 1994), $7.58^{+0.025}_{-0.026}$ (Kobulnicky & Skillman 1996), 7.52±0.01 (Fricke et al. 2001). In Tol 65 we derive an oxygen abundance 12 + log (O/H) = 7.54 ± 0.01 which is in agreement with 7.53±0.05 (Kunth & Sargent 1983), 7.42±0.07 (Campbell et al. 1986), 7.59±0.05 (Pagel et al. 1992), 7.40 – 7.54 (Masegosa et al. 1994), $7.56^{+0.032}_{-0.033}$ (Kobulnicky & Skillman 1996).

The spectral resolution of the Tol 1214–277 spectrum is not enough to measure the flux of the weak [N II] λ6583 which is contaminated by the Hα emission line. Therefore, to derive the nitrogen abundance we use the [N II]/Hα flux ratio obtained by Pagel et al. (1992) from a higher resolution spectrum. We obtain log N/O = –1.64±0.02. This value is lower than previous values of –1.46±0.06 (Pagel et al. 1992) and $-1.45^{+0.080}_{-0.098}$ (Kobulnicky & Skillman 1996). The difference in N/O comes mainly from the differing fluxes of [O II] λ3727 emission line. This line is used for determination of the ionization correction factor for nitrogen and it varies from $I(\lambda3727)/I(H\beta)$ = 0.23 (Pagel et al. 1992) to 0.34 in this paper, the difference being 0.17 dex. Fricke et al. (2001) derived log N/O = –1.50±0.02 from VLT observations. However, no flux calibration was available for those observations and hence Fricke et al. (2001) used earlier spectroscopic observations of Tol 1214–277 with the KPNO 2.1m telescope to calibrate their VLT spectrum. The [N II] λ6583 emission line is stronger in the spectrum of Tol 65 and we derive log N/O = –1.64 ± 0.02. All other log N/O values for Tol 65 are derived from a single observation by Kunth & Sargent (1983) who obtained log N/O = –1.75 ± 0.07, while Pagel et al. (1992) quote –1.81±0.15, and Kobulnicky & Skillman (1996) quote $-1.79^{+0.15}_{-0.23}$. Our value of log N/O in Tol 65 obtained

from the high signal-to-noise ratio spectrum is the same as that derived for Tol 1214–277 and is very close to the mean value of –1.60, derived for the most metal-deficient galaxies with 12 + log O/H < 7.6 (Thuan et al. 1995; Izotov & Thuan 1999), further supporting the very low dispersion of the N/O ratio in those galaxies. Such a constant N/O abundance ratio in the lowest-metallicity BCDs favors primary production of nitrogen in massive stars (Izotov & Thuan 1999) and may have important implications for analysis of the abundance patterns in high-redshift damped Lyα systems (Izotov, Schaerer & Charbonnel 2001).

The element-to-oxygen abundance ratios in Tol 1214–277 and Tol 65 for α-product elements are the same within the errors (Table 2) and they are close to the mean values derived for low-metallicity BCDs (Izotov & Thuan 1999). The exception is iron. While the Fe/O abundance ratio in Tol 65, though slightly lower, is consistent with the mean value for BCDs (Izotov & Thuan 1999), the Fe/O abundance ratio in Tol 1214–277 is 2σ larger. A similar Fe/O abundance ratio was found by Izotov et al. (1997, 1999) for the BCD SBS 0335–052 and was interpreted to be a result of the contamination of the [Fe III] λ4658 emission line by stellar or nebular C IV λ4658 line emission. This interpretation seems to be likely, because both SBS 0335–052 and Tol 1214–277 are galaxies with the strongest nebular He II λ4686 emission lines, implying very hard ionizing radiation. Only in those two BCDs was the [Fe V] λ4227 emission line detected, again supporting the presence of hard radiation (Fricke et al. 2001). Our derived abundance of O^{+3} in Tol 1214–277 is 5.5% of the total oxygen abundance (Table 2). Hence we expect that a significant amount of carbon in the H II region is present in the form of C^{3+}, implying the presence of C IV λ4658 line emission.

4. Helium abundance

He I emission-line fluxes are converted to singly ionized helium abundances $y^+ \equiv He^+/H^+$ using theoretical He I recombination line emissivities by Smits (1996). However, collisional and fluorescent enhancements can cause the observed He I fluxes to deviate from recombination values. In order to correct for these effects, we have adopted the following procedure, discussed in more detail in ITL94 and ITL97. We evaluate the electron number density N_e(He II) and the optical depth $\tau(\lambda3889)$ in the He I λ3889 line in a self-consistent way, so that the He I $\lambda\lambda$3889/5876, 4471/5876, 6678/5876 and 7065/5876 line ratios have their recombination values, after correction for collisional and fluorescent enhancement. Corrections are determined using the formulae by Kingdon & Ferland (1995) for collisional enhancement and the Izotov & Thuan (1998) fits to Robbins (1968) calculations for fluorescent enhancement. The He I λ3889 and 7065 lines play an important role because they are particularly sensitive to both optical depth and electron number density. Since the He I λ3889 line

is blended with the H8 λ3889 line, we have subtracted the latter, assuming its intensity to be equal to 0.106 $I(\mathrm{H}\beta)$ (Aller 1984), after correction for interstellar extinction and underlying stellar absorption in hydrogen lines. The singly ionized helium abundance y^+ and ^{4}He mass fraction Y is obtained for each of the three He I lines $\lambda\lambda$ 4471, 5876 and 6678. We then derive the weighted mean y^+ of these three determinations, the weight of each line being determined by its intensity. However, this weighted mean value may be underestimated due to the lower value of $y^+(4471)$ resulting from underlying stellar absorption. Therefore, in subsequent discussions we also use the weighted mean values of Y derived from the intensities of only two lines, He I λ5876 and λ6678 Å.

Additionally, we have added to y^+ the abundance of doubly ionized helium y^{+2} which is derived from the He II λ4686 Å emission line flux. Finally the helium mass fraction is calculated as

$$Y = \frac{4y[1 - 20(\mathrm{O/H})]}{1 + 4y}, \tag{3}$$

where $y = y^+ + y^{+2}$ is the number density of helium relative to hydrogen (Pagel et al. 1992).

The results of the ^{4}He abundance determination are presented in Table 3, where we show the adopted electron temperature T_e and the derived electron number density N_e in the He^+ zone, the optical depth in the He I λ3889 emission line, ionic abundances y^+ and y^{+2}, total abundances y and helium mass fractions Y derived for each line and the two weighted means. The errors in T_e(O III) and N_e (He II) are propagated in calculations of the helium mass fractions Y. The helium mass fraction in Tol 1214–277 is slightly lower for the He I λ4471 emission line, which is most subject to underlying stellar absorption. Similarly, systematically lower Y from the He I λ4471 emission line was derived earlier in two BCDs, SBS 0335–052 ($Z_\odot$/40, Izotov et al. 1999) and SBS 0940+544 ($Z_\odot$/27, Guseva et al. 2001), observed with Keck. The contribution of the doubly ionized He in Tol 1214–277 is significant and amounts to 6% of the total He abundance. Earlier, Fricke et al. (2001) arrived at the same conclusion for this BCD. The helium mass fraction in Tol 1214–277 is $Y = 0.2458 \pm 0.0039$ when all three lines are used, and 0.2466 ± 0.0043 when the He I λ4471 emission line is excluded. The effect of the underlying stellar absorption is more significant in Tol 65. The helium mass fraction Y derived from the He I λ4471 emission line is $\sim 10\%$ lower than that derived from other lines. The contribution of doubly ionized helium in Tol 65 is smaller than that in Tol 1214–277 and amounts to $\sim 1.4\%$ of the total helium abundance. The helium mass fraction in Tol 65 is $Y = 0.2410 \pm 0.0050$ when all three lines are used, and 0.2463 ± 0.0057 when the He I λ4471 emission line is excluded. Because of the effect of underlying absorption in the He I λ4471 emission line, we finally adopt for Tol 1214–277 and Tol 65 respectively $Y = 0.2466 \pm 0.0043$ and 0.2463 ± 0.0057. These values are very similar to 0.2463 ± 0.0015 in SBS 0335–052 (Izotov et al. 1999) and 0.2468 ± 0.0034 in SBS

0940+544 (Guseva et al. 2001) derived from the analysis of high signal-to-noise ratio Keck spectra.

5. Systematic effects

The similarity of Y in the lowest-metallicity BCDs suggests that statistical errors in the helium abundance determination are small. However, some systematic effects may change the value of Y. We already pointed out one such effect, the underlying stellar absorption, which if not accounted for, results in the underestimation of Y. This effect is more pronounced for the He I λ4471 emission line. Recently, González Delgado, Leitherer & Heckman (1999) have produced synthetic spectra of H Balmer and He I absorption lines in starburst and poststarburst galaxies. They predict that the equivalent width of the He I λ4471 absorption line for young starbursts with an age $t \lesssim 5$ Myr, which is the case for Tol 1214–277 and Tol 65, can be in the range 0.4 – 0.6 Å. Comparing with equivalent widths of the He I λ4471 emission line 7.6Å and 4.8Å in Tol 1214–277 and Tol 65, we conclude that the underestimate of the He abundance can be as high as $\sim 10\%$ in the case of the He I λ4471 emission line. For the other two He I lines λ5876 and λ6678 lines the underestimate seems to be significantly smaller because of larger emission line equivalent widths. Unfortunately, González Delgado et al. (1999) did not calculate equivalent widths for the He I λ5876 and λ6678 absorption lines. The weighted mean helium mass fraction in our calculations is mainly defined by the strongest He I λ5876 emission line with the highest weight. The upward correction of Y for this line due to the underlying stellar absorption is not larger than $\sim 1\%$ for Tol 1214–277 and $\sim 1\%$ – 2% for Tol 65. Here we assume that the equivalent width of the He I λ5876 absorption line is 0.4Å, which is ~ 100 times smaller than the equivalent width of the emission line in Tol 1214–277 and ~ 80 times smaller in Tol 65 (Table 1).

Another source of systematic uncertainties comes from the assumption that the H^+ and He^+ zones in the H II region are coincident. However, depending on the hardness of the ionizing radiation, the radius of the He^+ zone can be smaller than the radius of the H^+ zone in the case of soft ionizing radiation and larger in the case of hard radiation. In the former case, a correction for unseen neutral helium should be made, resulting in an ionization correction factor $ICF(\mathrm{He}) > 1$ and hence a higher helium abundance. In the latter case, the situation is opposite and $ICF(\mathrm{He}) < 1$. Furthermore, the electron temperature T_e in the O^{+2} zone derived from the collisionally excited [O III] lines was assumed in our calculations to be constant and is the same as that in the H^+ and He^+ zones. However, T_e(O III) tends to be larger than the temperature for the recombination lines of H I and He II and, if applied, results in an overestimate of the helium abundance. Both these effects have been discussed in

several studies (e.g., Pagel et al. 1992; ITL97; Steigman, Viegas & Gruenwald 1997; Olive et al. 1997; Viegas et al. 2000; Peimbert, Peimbert & Ruiz 2000; Ballantyne et al. 2000; Sauer & Jedamzik 2001). It was shown that the correction of the helium abundance can be as high as several percent in either downward or upward directions depending on the hardness of the radiation. The hardness is characterized by the "radiation softness parameter" η defined by Vílchez & Pagel (1988) as

$$\eta = \frac{\mathrm{O}^{+}}{\mathrm{S}^{+}} \frac{\mathrm{S}^{+2}}{\mathrm{O}^{+2}}. \quad (4)$$

Besides η some other parameters have been used to derive ICF(He), in particular the [O III] λ5007/Hβ and [O III] λ5007/[O I] λ6300 emission line flux ratios (Ballantyne et al. 2000), the ionization parameter U, which is the ratio of ionizing photon density to gas density, and the combination of all preceeding parameters (Sauer & Jedamzik 2001).

Sauer & Jedamzik (2001) calculated an extensive grid of photoionized H II region models aiming to derive the correction factors as functions of η and U. Their conclusion was that a downward correction of Y as much as 6% and 2% is required respectively for ionization parameters log U = –3.0 and –2.5 (see their Fig. 18). However, the downward correction is $\lesssim$ 1% if log $U \gtrsim$ –2.0.

For Tol 1214–277 and Tol 65 we find respectively log η = –0.29 and –0.08. The ratios ([O III] λ4959 + 5007)/[O II] λ3727 of 19.9 and 7.2 in those galaxies (Table 1) at an oxygen abundance 12 + log O/H = 7.54 correspond to an ionization parameter log $U \gtrsim$ –2.0 (McGaugh 1991). In particular, Campbell (1988) derived log $U = -1.61^{+0.10}_{-0.43}$ for Tol 1214–277 at the 70% confidence level. With these η and U values, the downward correction of Y due to ionization effects and variations of the electron temperature in Tol 1214–277 and Tol 65 is unlikely to be greater than $\sim$ 1%. Taking into account the fact that the upward correction of Y due to underlying stellar absorption can be as high as 1% – 2%, we conclude that both effects seem to offset each other and the combined systematic uncertainty is $\lesssim$ 1% in Tol 1214–277 and Tol 65. Similar conclusions can be drawn for SBS 0335–052 (Izotov et al. 1999) and SBS 0940+544 (Guseva et al. 2001).

Another approach has been developed by Peimbert (1967) to take into account the difference in the electron temperature in the O^{++} zone as compared to the H^{+} and He^{+} zones. He developed a formalism introducing an average temperature T_0 and a mean square temperature variation t^2 in an H II region. Then the temperatures in the O^{++} and H^{+} and He^{+} zones are expressed as different functions of T_0 and t^2, and in hot H II regions T_e(O III) $\geq$ T_e(H II), T_e(He II). This approach has been applied by Peimbert et al. (2001) for the determination of the He abundance in some low-metallicity dwarf galaxies, including the two most-metal deficient BCDs, I Zw 18 and SBS 0335–052. They use the observations by Izotov et al. (1999) and find that while the ionization correction factors ICF(He) in

both galaxies are very close to unity, the difference in T_e(O III) and T_e(He II) results in the reduction of the He mass fraction by 2 – 3 percent compared to the case with T_e(O III) = T_e(He II). Additionally, Peimbert et al. (2001) considered the effect of collisional excitation of hydrogen emission lines, first noted by Davidson & Kinman (1985). Neglecting this effect results in an artificially large extinction and hence overcorrection of the He I λ5876 and λ6678 emission lines. Peimbert et al. (2001) find that this effect in I Zw 18 and SBS 0335–052 leads to an the upward correction of Y by $\sim$ 2%. Hence, after correction for all the systematic effects considered, they obtain $Y = 0.241$ and 0.245, respectively for I Zw 18 and SBS 0335–052. These values are similar to $Y = 0.243$ and 0.246 derived earlier by Izotov et al. (1999) for those galaxies. The importance of the correction for collisional excitation of the hydrogen emission lines has been pointed out also by Stasińska & Izotov (2001) who concluded that this effect can result in an upward Y correction of up to 5%, assuming that the excess of the Hα/Hβ flux ratio above the theoretical recombination value is due only to collisional excitation. However, in practice, some part of the Hα/Hβ flux ratio excess is due to interstellar extinction and the correction of Y for collisional excitation of the hydrogen lines is likely smaller, only $\sim$ 2 – 3 percent, similar to the value obtained by Peimbert et al. (2001). Because the physical conditions in the H II regions of SBS 0940+544 (Guseva et al. 2001), Tol 1214–277 and Tol 65 (this paper) are similar to those in I Zw 18 and SBS 0335–052, we expect that the estimates above for the systematic errors are valid for all the very metal-deficient high-excitation H II regions considered in this paper.

Besides the above effects, the uncertainties in the He I recombination coefficients of $\sim$ 1.5% also may play a role (Benjamin, Skillman & Smits 1999). Although some systematic effects are still difficult to estimate and are poorly studied, when taken into account together, it seems that they largely offset each other. Because of the uncertainties of these effects, we conservatively assume that combined systematic error in the He abundance determination may be tentatively set to 2% (the error is 2σ).

Our studies show that the helium mass fraction in the lowest-metallicity BCDs observed with the Keck telescope lies in the range 0.246 – 0.247. Correction for the small contribution of ^{4}He produced in stars $\Delta Y = 0.0010 - 0.0017$ (Izotov et al. 1999), results in a mean primordial ^{4}He mass fraction $Y_{\rm p}$ of 0.245 $\pm$ 0.003 (rms) $\pm$ 0.005(sys) (2σ) obtained from the Keck observations of the four galaxies, in agreement with the previous studies of ITL97, Izotov & Thuan (1998) and Izotov et al. (1999). This $Y_{\rm p}$ predicts a baryon mass fraction $\Omega_{\rm b}h^2 = 0.017\pm0.005({\rm rms})^{+0.010}_{-0.007}({\rm sys})$ (2σ), consistent with 0.020$\pm$0.002 (2σ) derived from the primordial deuterium abundance (Burles & Tytler 1998a, 1998b; Burles et al. 2001). It is also consistent with the estimation of high-ℓ peaks in the angular power spectrum of the Cosmic Microwave Background (CMB) (Netterfield et al. 2001). This overall consistency gives uniform support to the standard big bang nucleosynthesis model. In particular, if the

baryon mass fraction $\Omega_{\rm b}h^2 = 0.022\pm0.003$ (1σ) inferred from the CMB power spectrum is adopted, then, in the frame of the SBBN, the predicted primordial ^{4}He mass fraction is $Y_{\rm p} = 0.248\pm0.001$ (Lopez & Turner 1999; Burles, Nollett & Turner 2001). Our $\Omega_{\rm b}h^2$ is also consistent with $\Omega_{\rm b}h^2 = 0.025\pm0.001$ (1σ) derived by Pettini & Bowen (2001) from the deuterium abundance measurements in the $z_{\rm abs} = 2.0762$ damped Lyman α system toward the QSO 2206–199 if 2σ systematic error of 2% in $Y_{\rm p}$ is assumed.

6. Summary

The main conclusions drawn from our Keck spectroscopic analysis of the extremely metal-deficient BCDs Tol 1214–277 and Tol 65 may be summarized as follows:

1. The oxygen abundances in Tol 1214–277 and Tol 65 are 12 + log O/H = 7.54 ± 0.01, or 1/24 solar. We find that the nitrogen-to-oxygen abundance ratio in both galaxies is log N/O = –1.64 ± 0.02, close to the mean value of –1.60 found for the other most-metal deficient BCDs with $Z < Z_{\odot}/20$ (Thuan et al. 1995; Izotov & Thuan 1999). Alpha-product element-to-oxygen abundance ratios are in the same range as those found for BCDs. The exception is the apparently higher Fe/O abundance ratio in Tol 1214–277 which we argue is due to the contamination of [Fe III] λ4658 emission line by C IV λ4658 emission.

2. The ^{4}He mass fractions in Tol 1214–277 and Tol 65 are respectively $Y = 0.2466\pm0.0043$ and 0.2463 ± 0.0057. These values, after small corrections for the helium produced in stars, correspond to a primordial ^{4}He mass fraction of 0.245, in excellent agreement with previous studies of ITL97, Izotov & Thuan (1998) and Izotov et al. (1999), supporting the validity of the standard big bang nucleosynthesis model.

3. We find that the systematic uncertainties in the ^{4}He abundance determination in Tol 1214–277 and Tol 65 due to the combined effect of underlying stellar absorption, temperature and ionization structure of the H II region and collisional excitation of the hydrogen emission lines are likely small, not exceeding $\sim 2\%$ (2σ).

Y.I.I. thanks for partial financial support through NATO grant PST.EV.976026, Swiss SCOPE grant 7UKRJ62178 and for hospitality at National Optical Astronomical Observatory.

REFERENCES

Aller, L. H. 1984, Physics of Thermal Gaseous Nebulae (Dordrecht: Reidel)

Ballantyne, D. R., Ferland, G. J., & Martin, P. G. 2000, ApJ, 536, 773

Benjamin, R. A., Skillman, E. D., & Smits, D. P. 1999, ApJ, 514, 307

Bohlin, R. C. 1996, AJ, 111, 1743

Burles, S., Nollett, K. M., & Turner, M. S. 2001, ApJ, 552, L1

Burles, S., & Tytler, D. 1998a, ApJ, 499, 699

———. 1998b, ApJ, 507, 732

Campbell, A. 1988, ApJ, 335, 644

Campbell, A., Terlevich, R., & Melnick, J. 1986, MNRAS, 223, 811

Davidson, K., & Kinman, T. D. 1985, ApJS, 58, 321

Filippenko, A. V. 1982, PASP, 94, 715

Fricke, K. J., Izotov, Y. I., Papaderos, P., Guseva, N. G., & Thuan, T. X. 2001, AJ, 121, 169

Garnett, D. R. 1992, AJ, 103, 1330

González Delgado, R., Leitherer, C., & Heckman, T. M. 1999, ApJS, 125, 489

Guseva, N. G., Izotov, Y. I., Papaderos, P., et al. 2001, A&A, in press

Izotov, Y. I., Chaffee, F. H., Foltz, C. B., Green, R. F., Guseva, N. G., & Thuan, T. X. 1999, ApJ, 527, 757

Izotov, Y. I., Lipovetsky, V. A., Chaffee, F. H., et al. 1997, ApJ, 476, 698

Izotov, Y. I., Schaerer, D., & Charbonnel, C. 2001, ApJ, 549, 878

Izotov, Y. I., & Thuan, T. X. 1998, ApJ, 500, 188

———. 1999, ApJ, 511, 639

Izotov, Y. I., Thuan, T. X., & Lipovetsky, V. A. 1994, ApJ, 435, 647 (ITL94)

———. 1997c, ApJS, 108, 1 (ITL97)

Kingdon, J., & Ferland, G. J. 1995, ApJ, 442, 714

Kobulnicky, H. A., & Skillman, E. D. 1996, ApJ, 471, 211

Kunth, D., & Sargent, W. L. W. 1983, ApJ, 273, 81

Lopez, R. E., & Turner, M. S. 1999, Phys. Rev. D, 59, 103502

Masegosa, J., Moles, M., & Campos-Aguilar, A. 1994, ApJ, 420, 576

McGaugh, S. S. 1991, ApJ, 380, 140

Netterfield, C. B., et al. 2001, ApJ, in press; preprint astro-ph/0104460

Oke, J. B. 1990, AJ, 99, 1621

Oke, J. B., et al. 1995, PASP, 107, 375

Olive, K. A., Steigman, G., & Skillman, E. D. 1997, ApJ, 483, 788

Pagel, B. E. J. 2000, Phys. Rep., 333, 433

Pagel, B. E. J., Simonson, E. A., Terlevich, R. J., & Edmunds, M. G. 1992, MNRAS, 255, 325

Pagel, B. E. J., Terlevich, R. J., & Melnick, J. 1986, PASP, 98, 1005

Peimbert, M. 1967, ApJ, 150, 825

Peimbert, A., Peimbert, M., & Luridiana, V. 2001, ApJ, in press; preprint astro-ph/0107189

Peimbert, M., Peimbert, A., & Ruiz, M. 2000, ApJ, 541, 688

Peimbert, M., & Torres-Peimbert, S. 1974, ApJ, 193, 327

———. 1976, ApJ, 203, 581

Pettini, M., & Bowen, D. V. 2001, ApJ, in press; preprint astro-ph/0104474

Robbins, R. R. 1968, ApJ, 151, 511

Sauer, D., & Jedamzik, K. 2001, A&A, in press; preprint astro-ph/0104392

Smits, D. P. 1996, MNRAS, 278, 683

Stasińska, G. 1990, A&AS, 83, 501

Stasińska, G., & Izotov, Y. I. 2001, A&A, in press

Steigman, G., Viegas, S. M., & Gruenwald, R. 1997, ApJ, 490, 187

Thuan, T. X., Izotov, Y. I., & Lipovetsky, V. A. 1995, ApJ, 445, 108

Viegas, S., Gruenwald, R., & Steigman, G. 2000, ApJ, 531, 813

Vílchez, J. M., & Pagel, B. E. J. 1988, MNRAS, 231, 257

Table 1. Emission line fluxes and equivalent widths

Ion	Tol 1214–277			Tol 65		
	$F(\lambda)/F(\mathrm{H}\beta)$	$I(\lambda)/I(\mathrm{H}\beta)$	EW	$F(\lambda)/F(\mathrm{H}\beta)$	$I(\lambda)/I(\mathrm{H}\beta)$	EW
3727 [O II]	0.332±0.006	0.341±0.006	42.3	0.634±0.010	0.674±0.011	67.1
3750 H12	0.031±0.002	0.033±0.003	4.1	0.012±0.001	0.046±0.007	1.3
3770 H11	0.034±0.002	0.035±0.003	4.5	0.024±0.002	0.059±0.005	2.7
3798 H10	0.050±0.002	0.052±0.003	6.8	0.033±0.002	0.068±0.004	3.6
3835 H9	0.052±0.002	0.054±0.003	7.1	0.046±0.002	0.082±0.004	4.9
3868 [Ne III]	0.343±0.006	0.351±0.006	47.3	0.246±0.004	0.259±0.005	26.1
3889 He I + H8	0.203±0.004	0.208±0.004	28.2	0.154±0.003	0.197±0.004	16.2
3968 [Ne III] + H7	0.291±0.005	0.298±0.005	43.3	0.208±0.004	0.251±0.005	21.9
4026 He I	0.019±0.001	0.019±0.001	3.0	0.012±0.002	0.013±0.002	1.3
4069 [S II]	0.008±0.001	0.008±0.001	1.2	0.011±0.002	0.011±0.002	1.2
4101 Hδ	0.268±0.005	0.274±0.005	45.6	0.222±0.004	0.260±0.005	25.8
4227 [Fe V]	0.007±0.001	0.007±0.001	1.3	···	···	···
4340 Hγ	0.481±0.008	0.488±0.008	96.9	0.443±0.007	0.477±0.008	58.0
4363 [O III]	0.167±0.003	0.169±0.003	34.0	0.093±0.002	0.095±0.002	12.3
4471 He I	0.035±0.001	0.035±0.001	7.6	0.034±0.002	0.034±0.002	4.8
4658 [Fe III]	0.005±0.001	0.005±0.001	1.2	0.006±0.001	0.006±0.001	1.0
4686 He II	0.049±0.002	0.049±0.002	12.1	0.012±0.001	0.012±0.001	1.9
4711 [Ar IV] + He I	0.027±0.001	0.027±0.001	6.7	0.011±0.001	0.011±0.001	1.8
4740 [Ar IV]	0.016±0.001	0.016±0.001	4.0	0.006±0.001	0.006±0.001	0.9
4861 Hβ	1.000±0.015	1.000±0.015	267.5	1.000±0.015	1.000±0.015	174.1
4922 He I	0.012±0.001	0.012±0.001	3.2	0.011±0.001	0.010±0.001	1.9
4959 [O III]	1.707±0.025	1.703±0.025	478.3	1.243±0.019	1.212±0.018	225.7
5007 [O III]	5.100±0.075	5.082±0.075	1467.2	3.733±0.055	3.628±0.055	693.4
5200 [N I]	···	···	···	0.007±0.001	0.007±0.001	1.4
5876 He I	0.093±0.002	0.091±0.002	41.4	0.111±0.002	0.103±0.002	31.4
6300 [O I]	0.012±0.001	0.011±0.001	6.1	0.020±0.001	0.019±0.001	6.7
6312 [S III]	0.008±0.001	0.008±0.001	4.2	0.011±0.001	0.010±0.001	3.8
6363 [O I]	0.003±0.001	0.003±0.001	1.5	0.008±0.001	0.007±0.001	2.6
6563 Hα	2.822±0.042	2.737±0.044	1571.1	3.074±0.045	2.769±0.045	1079.6
6583 [N II]	···	···	···	0.020±0.001	0.018±0.001	4.7

Table 1—Continued

Ion	Tol 1214–277			Tol 65		
	$F(\lambda)/F(\mathrm{H}\beta)$	$I(\lambda)/I(\mathrm{H}\beta)$	EW	$F(\lambda)/F(\mathrm{H}\beta)$	$I(\lambda)/I(\mathrm{H}\beta)$	EW
6678 He I	0.026±0.001	0.025±0.001	15.4	0.031±0.001	0.027±0.001	11.2
6717 [S II]	0.024±0.001	0.023±0.001	14.1	0.071±0.002	0.064±0.002	26.7
6731 [S II]	0.021±0.001	0.020±0.001	12.7	0.052±0.001	0.046±0.001	19.7
7065 He I	0.025±0.001	0.024±0.001	17.1	0.031±0.001	0.028±0.001	13.6
7135 [Ar III]	0.022±0.001	0.022±0.001	15.6	0.035±0.001	0.031±0.001	15.7
7281 He I	0.006±0.001	0.005±0.001	4.0	0.006±0.001	0.005±0.001	2.9
7320 [O II]	0.005±0.001	0.005±0.001	3.8	0.016±0.001	0.014±0.001	7.6
7330 [O II]	0.004±0.001	0.004±0.001	3.0	0.011±0.001	0.010±0.001	5.4
$C(\mathrm{H}\beta)$ dex	0.040±0.019			0.115±0.019		
$F(\mathrm{H}\beta)$[a]	1.88±0.01			2.65±0.01		
EW(abs) Å	0.1			3.5		

[a]in units of 10^{-14} erg s^{-1}cm^{-2}.

Table 2. Heavy element abundances

Parameter	Tol 1214–277	Tol 65
T_e(O III)(K)	19790±260	17320±240
T_e(O II)(K)	15630±190	14770±200
T_e(S III)(K)	18130±210	16080±200
N_e(S II)(cm^{-3})	400±120	50±50
$O^+/H^+(\times10^5)$	0.273±0.010	0.614±0.024
$O^{+2}/H^+(\times10^5)$	2.982±0.095	2.816±0.101
$O^{+3}/H^+(\times10^5)$	0.191±0.011	0.046±0.005
$O/H(\times10^5)$	3.447±0.096	3.477±0.104
12 + log(O/H)	7.538±0.012	7.541±0.013
$N^+/H^+(\times10^7)$	···	1.402±0.065
ICF(N)[a]	···	5.66
log(N/O)	···	–1.642±0.024
$Ne^{+2}/H^+(\times10^5)$	0.418±0.014	0.425±0.016
ICF(Ne)[a]	1.16	1.23
log(Ne/O)	–0.854±0.019	–0.821±0.021
$S^+/H^+(\times10^7)$	0.414±0.014	1.118±0.031
$S^{+2}/H^+(\times10^7)$	2.304±0.228	4.272±0.353
ICF(S)[a]	2.90	1.69
log(S/O)	–1.640±0.039	–1.581±0.031
$Ar^{+2}/H^+(\times10^7)$	0.576±0.024	0.981±0.036
$Ar^{+3}/H^+(\times10^7)$	1.252±0.087	0.596±0.129
ICF(Ar)[a]	1.01	1.03
log(Ar/O)	–2.273±0.025	–2.332±0.039
$Fe^{+2}/H^+(\times10^7)$	0.864±0.222[b]	1.187±0.274
ICF(Fe)[a]	15.8	7.07

Table 2—Continued

Parameter	Tol 1214–277	Tol 65
log(Fe/O)	–1.404±0.112[b]	–1.617±0.101
[O/Fe]	–0.017±0.112	0.197±0.101

[a]ICF is the ionization correction factor for unseen stages of ionization. The expressions for ICFs are adopted from ITL94.

[b]Probable overestimate; see text.

Table 3. Helium abundance

Parameter	Tol 1214–277	Tol 65
T_e(O III)(K)	19790±260	17320±240
N_e(He II)(cm^{-3})	25±1	150±50
$\tau(\lambda3889)$	0.01	0.01
$y^+(\lambda4471)$	0.0755±0.0029	0.0706±0.0033
$y^+(\lambda5876)$	0.0773±0.0016	0.0812±0.0022
$y^+(\lambda6678)$	0.0773±0.0028	0.0796±0.0031
y^+(weighted mean)	0.0770±0.0013	0.0784±0.0016
$y^+(\lambda5876 + \lambda6678)$	0.0773±0.0014	0.0807±0.0018
$y^{+2}(\lambda4686)$	0.0046±0.0001	0.0011±0.0001
$y(\lambda4471)$	0.0801±0.0029	0.0717±0.0033
$y(\lambda5876)$	0.0819±0.0016	0.0823±0.0022
$y(\lambda6678)$	0.0819±0.0028	0.0796±0.0031
y(weighted mean)	0.0816±0.0013	0.0795±0.0016
$y(\lambda5876 + \lambda6678)$	0.0819±0.0014	0.0818±0.0018
$Y(\lambda4471)$	0.2424±0.0090	0.2226±0.0107
$Y(\lambda5876)$	0.2466±0.0050	0.2475±0.0069
$Y(\lambda6678)$	0.2466±0.0087	0.2439±0.0098
Y (weighted mean)	0.2458±0.0039	0.2410±0.0050
Y ($\lambda5876 + \lambda6678$)	0.2466±0.0043	0.2463±0.0057

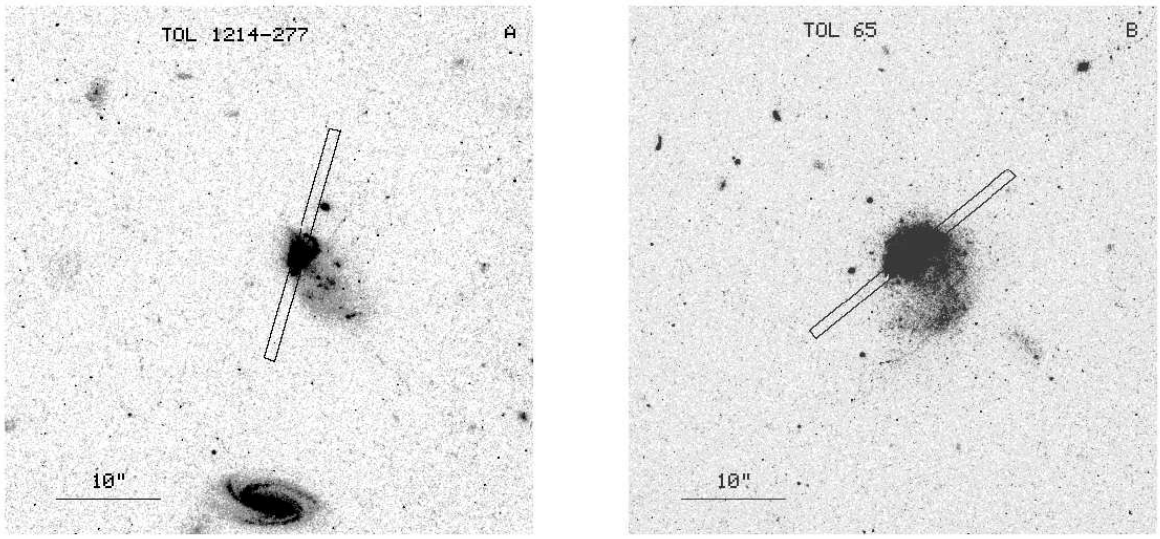

Fig. 1.— The archival *Hubble Space Telescope V* images of Tol 1214–277 (a) and Tol 65 (b) with the orientation of the slit overplotted.

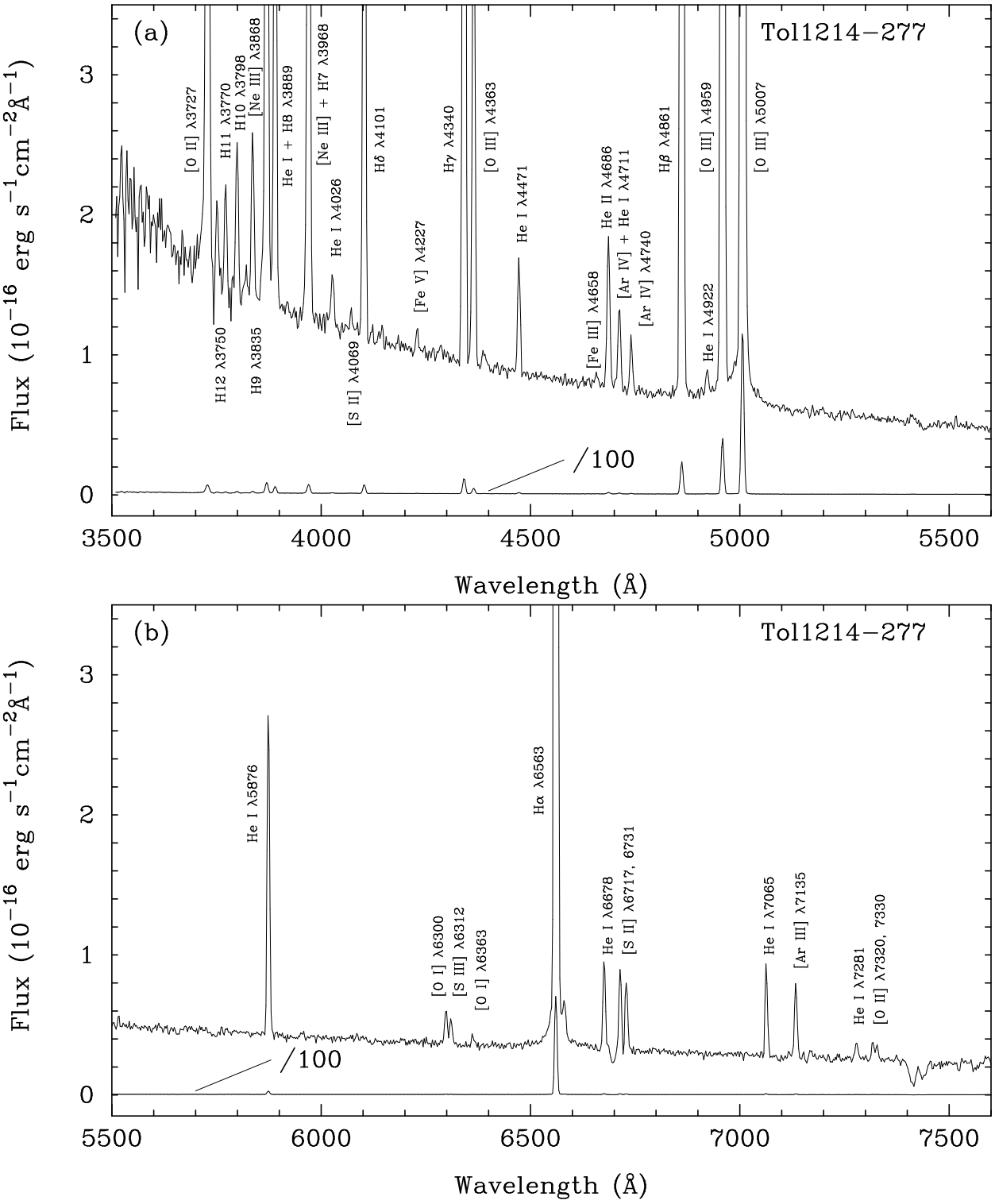

Fig. 2.— The spectrum of Tol 1214–277 in aperture $1'' \times 6''.8$. The lower spectrum is the observed spectrum downscaled by a factor of 100.

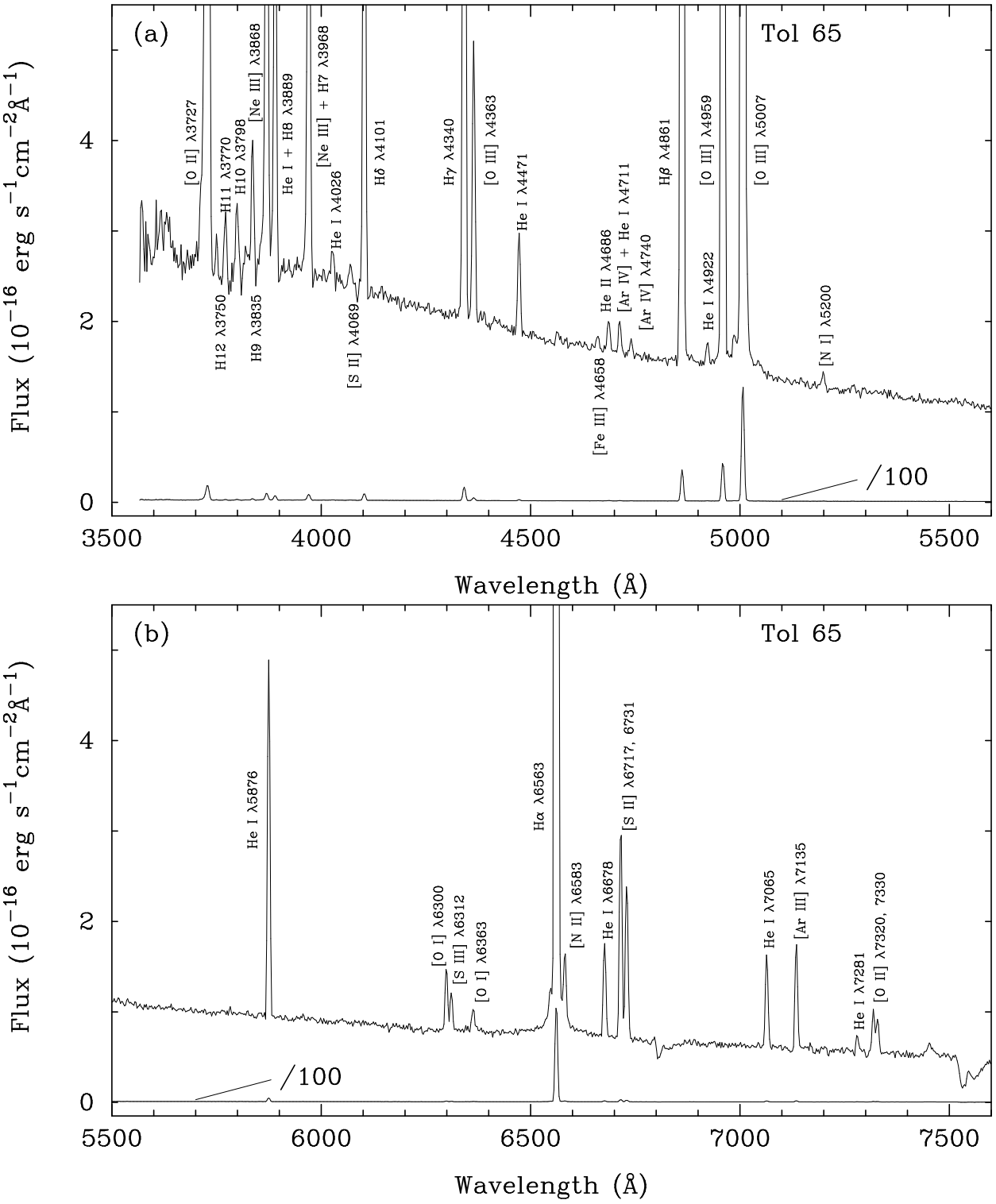

Fig. 3.— The spectrum of Tol 65 in aperture $1'' \times 8''.4$. The lower spectrum is the observed spectrum downscaled by a factor of 100.